Infrared thermal emission in macroporous silicon three-dimensional photonic crystals

M. Garín,[a] T. Trifonov, A. Rodríguez, and R. Alcubilla[b]
Departament d'Enginyeria Electrónica, Universitat Politècnica de Catalunya, Jordi Girona 1-3, Módul C4, 08034 Barcelona, Spain

(Received 30 July 2007; accepted 10 October 2007; published online 29 October 2007)

In this paper we investigate the infrared thermal emission properties of macroporous silicon with modulated pore diameter. Samples with different pore modulation periodicities but fixed in-plane lattice constant are fabricated. Normal emission of these samples is measured between 373 and 673 K. Room-temperature normal-incidence reflectance and transmission spectra are also measured and compared with the photonic band structure simulation. It is shown that thermal emission is suppressed due to photonic band gap effect along the pore axis in excellent agreement with the numerical calculations. © *2007 American Institute of Physics*. [DOI: 10.1063/1.2804002]

Tailoring of thermal emission spectrum through microfabrication of periodic structures has attracted great research interest for its potential application in lighting[1] and thermophotovoltaic energy conversion.[2] Three-dimensional (3D) photonic band gap (PBG) structures[3] are particularly flexible in managing and confining light in all three dimensions and, therefore, they are good candidates for controlling thermal radiation. Inside the photonic band gap region, thermal radiation from a PBG material can be fully inhibited due to the absence of photonic states. Conversely, outside the photonic band gap, emission can be enhanced due to an increase in the photonic density of states. Optical states can also be introduced inside the photonic band gap by creating defects in the lattice. Furthermore, surface modes can also be allowed by precise truncation of the crystal termination.[4] However, the fabrication of 3D PBG structures suitable for thermal radiation measurement is not easy, as they must be high quality, large area, and thermally stable structures. The unique experience up to now is the work of Lin *et al.*, which proposed woodpilelike silicon[5] and tungsten[2] 3D PBG structures. Silicon 3D structures[5] operate at infrared wavelengths, efficiently reducing Si emission inside the band gap and enhancing the emission outside it. Full-metallic tungsten PBG structures[2] exhibit wider band gaps, very selective emission, and are compatible with thermophotovoltaics applications. Woodpile PBG structures, however, have the disadvantage of needing a complex layer-by-layer fabrication process with precise alignment between PBG layers. These difficulties have motivated attempts to fabricate these structures by using soft lithography and metal electrodeposition techniques.[6]

An alternative way of fabricating 3D PBG structures is using macroporous silicon.[7] Macroporous silicon is a versatile material formed by electrochemical etching of *n*-type silicon wafers in hydrofluoric acid (HF) solutions. The sites where pores must grow are defined by standard lithography and structuring processes, making possible large-area high-quality 2D PBG structures.[8] Three-dimensional structures with pore diameter variation in depth are obtained by periodically varying the etching conditions. Specific postetching treatments, for example, oxidation/oxide removal steps, can connect the pores laterally improving the 3D symmetry and allowing a full photonic band gap.[9] In addition, line[10] and planar[11] defects can also be easily incorporated in those structures. The versatility of macroporous silicon makes it an interesting material for tailoring thermal emission in the infrared (IR) region. However, up to now, only 2D macroporous silicon has been used as IR source with blackbodylike behavior.[12]

In this article we study experimentally the thermal emission properties of 3D photonic crystals based on macroporous silicon with modulated pore diameter. These structures exhibit a photonic band gap in the longitudinal direction of the pores, which allows controlling thermal emission in the normal direction just by changing the pore modulation periodicity. Four periodicities, namely, 3, 4, 5, and 6 μm, of pore diameter modulation are investigated, while the in-plane periodicity remains constant. The samples are optically characterized by transmission and reflectance measurements at normal incidence together with numerical simulations of the optical band structure. Normal thermal emission of these structures has been measured between 373 and 673 K.

The procedure for sample preparation and electrochemical etching is given elsewhere,[13] the following is a brief description of the process. Base material is ⟨100⟩ oriented, single side polished, *n*-type, crystalline silicon wafers with a resistivity of 1–10 Ω cm and a thin n^+ doped layer on the backside as transparent Ohmic contact. First, the front surface of the sample is prestructured with a square array of inverted pyramids with a periodicity of 4 μm. Each pyramid defines the point where a pore will grow. The sample is then electrochemically etched under backside illumination in aqueous HF solution (5 wt %) with a small amount (0.1 mM) of TritonX-100 nonionic surfactant as wetting agent. During the electrochemical process, the illumination (and so the etching current) is varied periodically to introduce the pore diameter modulation. A sawtoothlike current profile was used in order to obtain sinusoidal-like modulated pores.[14] We have fabricated four samples with periodicities of 3, 4, 5, and 6 μm along the pore axis, all four with 21 crystal periods. To check the resulting profile, we have analyzed the final cross-sectional shape of the pores by scanning electron microscopy (SEM), as shown in Fig. 1(a). Figure 1(b) is a bird's eye view of one of the samples. The

[a]Electronic address: mgarin@eel.upc.edu
[b]Electronic address: alcubilla@eel.upc.edu

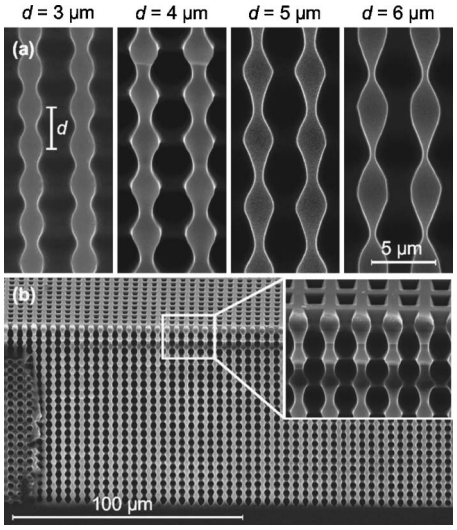

FIG. 1. Scanning electron microscopy (SEM) micrographs of the fabricated samples. (a) Cross-section view of the four fabricated samples. From left to right, the periodicities of the samples along the pore axis are 3, 4, 5, and 6 μm. (b) Bird's eye view of the sample with 4 μm periodicity.

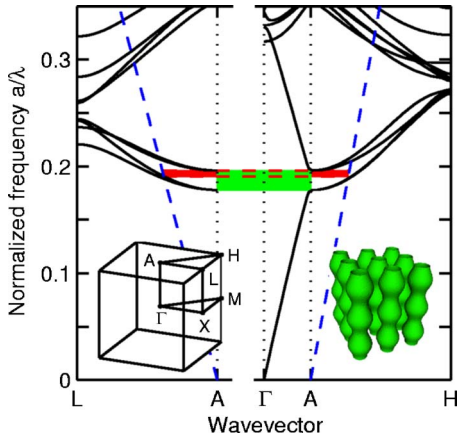

FIG. 2. (Color online) Photonic band dispersion of the 3D structure with modulated pores along with the light cone (dashed lines). Green region denotes the photonic band gap along the pore axis direction (Γ-*A* direction). Red colored region denotes the omnidirectional total reflection band. The left inset represents the irreducible Brillouin zone of the simple cubic lattice while the right inset is a 3D representation of the model used in the calculations.

averaged modulation periodicities measured from the SEM images are 2.87, 3.94, 5.01, and 5.91 μm, which are fairly close to the targeted ones. The attained pore diameter variation seen in the images is slightly lower as the periodicity is reduced. This effect arises from the dynamics of the pore growth and prevents the fabrication of samples with strongly modulated diameter for periods of modulation shorter than the in-plane periodicity.

The fabricated samples are square-lattice 3D periodic structures with fixed in-plane lattice constant a and variable periodicity d along the pore axis. We have performed numerical simulations of the photonic band structure using the free software MIT photonic-bands package.[15] An approximated three-dimensional model based on circular pores with sinusoidal modulation of pore radius with depth was used for the calculations (right inset in Fig. 2). The parameters for the model (maximum and minimum diameter and modulation periodicity) were derived from SEM micrographs of the fabricated samples. Figure 2 shows the calculated band diagram for the sample with 4 μm periodicity along with the light cone boundaries in dashed lines. Only the sections relevant to emission by the sample surface are represented. The structure does not have a complete 3D photonic band gap but it does present a forbidden gap (highlighted in green) in the pore axis direction, i.e., the Γ-*A* direction. Considering only the states that can couple with light traveling in vacuum, i.e., inside the light cone, the structure still presents a forbidden gap, hightlighted in red, known as omnidirectional total reflection band. As a totally reflective surface has zero emissivity, the structure can be practical for controlling emission in all directions, although postprocessed samples featuring complete photonic band gap[9] would exhibit better characteristics. Simulations for $d=5$ and 6 μm reveal a main photonic gap located at longer wavelengths and a secondary narrow gap at shorter wavelengths, while for $d=3$ μm a single photonic gap appear. At longer wavelengths, when $d>a$, the structure resembles a simple Bragg stack, thus explaining the observed several order band gaps. On the contrary, when $d\sim a$ or simply at shorter wavelengths, the lateral symmetry can no longer be neglected, which leads to a more complex band structure and prevents the expected higher order 1D band gaps from opening up.

Normal emittance spectra were measured using a Bruker Vertex 70 Fourier transform infrared (FT-IR) spectrometer equipped with a deuterated *L*-alanine doped triglycine sulfate (DLaTGS) detector, a KBr beamsplitter, and the emission adapter A540. The emission adapter allows measuring normal thermal emission spectra of solid samples from room temperature (293 K) up to 673 K. A conventional two-temperature calibration procedure[16] was conducted using a polished plate covered with a black organic film (emissivity $\varepsilon=95\%$) as a blackbody reference. After the calibration, the thermal emission spectra of all samples were acquired at four

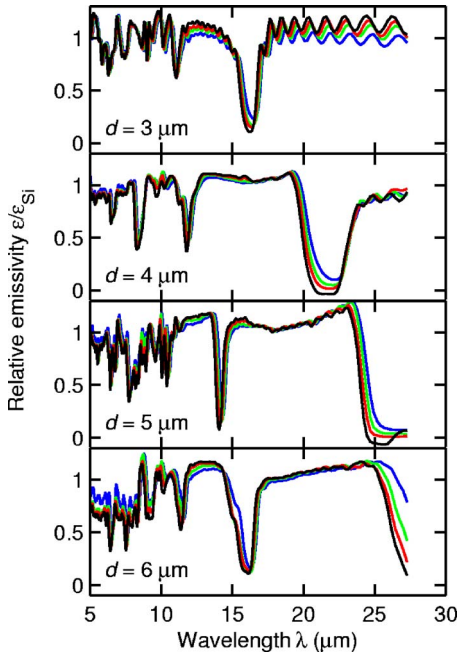

FIG. 3. (Color online) Normalized emittance spectra of 3D macroporous samples with periodicities along the pore axis of 3, 4, 5, and 6 μm. Black, red, green, and blue lines stand for the emittance measured at 373, 473, 573, and 673 K, respectively. Measurements are normalized to the emissivity of polished *n*-type Si.

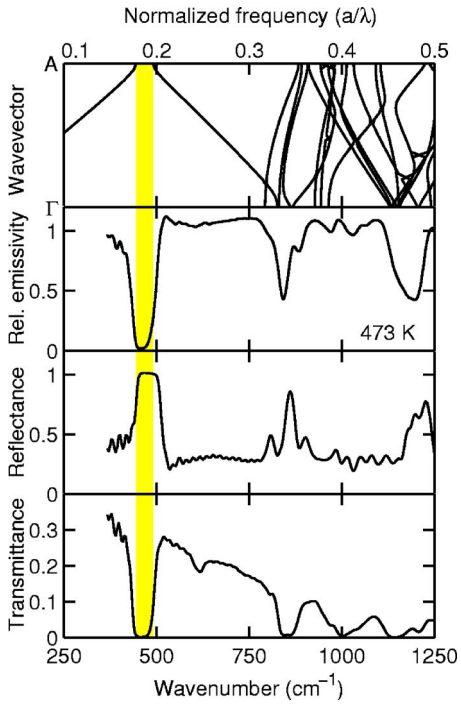

FIG. 4. (Color online) Comparison of normal emissivity, reflectance, and transmittance spectra with band structure calculation for the sample with 4 μm periodicity along the pore axis. The stop band is highlighted in yellow. Emissivity spectrum is measured at 473 K and is relative to polished *n*-Si emissivity. Reflectance spectrum is measured at a quasinormal incidence angle of 12°. Emissivity and transmittance spectra are measured at normal incidence.

temperatures between 373 and 673 K. We also measured at the same temperatures the emission spectrum from a piece of silicon with the same characteristics as the substrate used for the sample fabrication. All emissivity measurements are normalized to the emissivity of this silicon reference so that the effect of the structuring is emphasized over the bulk emission features. Figure 3 shows the relative normal emissivity spectra of the fabricated samples at temperatures of 373, 473, 573, and 673 K represented in black, red, green, and blue colors, respectively. Several spectral features, where emission is greatly reduced or inhibited, appear in the spectra. These features shift to shorter wavelengths as the modulation periodicity is reduced, in good agreement with calculated photonic gap behavior. First order band gap for samples with 5 and 6 μm periodicity could not be completely measured since it is at the edge of the measurable range. The second-order gap, however, can be clearly seen in both samples. As temperature increases, the effect of the band gap weakens due to increased free carrier absorption, while the spectral features slightly shift to longer wavelengths because of the increase in the silicon refractive index.

Additionally, we have performed room-temperature reflectance and transmittance measurements at quasinormal (12°) and normal incidence angles, respectively. A gold mirror was used as a reference for the reflectance measurements, while transmission data was normalized to the open beam spectrum. Since the backside n^+ layer, used for back contact, has a strong absorption coefficient in the mid-IR region, it was removed by reactive ion etching prior to the transmittance measurements. Figure 4 plots the emissivity spectra (at 473 K) for the 4 μm periodicity sample together with the measured reflectance, transmittance, and calculated photonic band dispersion along the Γ-*A* direction. The calculated gap nicely matches with the spectral region of zero emissivity, zero transmittance, and total reflectance, as expected. From these measurements Kirchhoff's emission law can also be verified. We will assume zero transmittance as it rapidly vanishes when the sample is heated, due to the increased free-carrier absorption. Under this assumption Kirchhoff's law states that $\varepsilon(\lambda)=1-r(\lambda)$, which is nicely fulfilled in the measurements owing to the highly symmetrical emissivity and reflectance spectra. The small deviations from Kirchhoff's law can be explained by the differences in angles and temperatures at which the reflectance and emissivity were measured.

We have presented 3D macroporous silicon as a selective thermal emitter in the mid-IR region. The 3D periodicity was obtained by periodically modulating the pore diameter during its formation. Measurements demonstrate that thermal emission is inhibited in the pore axis direction due to photonic band gap effect, in good agreement with numerical calculations. Progressive degradation of the photonic band gap effect and slight frequency shift to longer wavelengths have been observed as temperature is increased. The structure can be used to tailor emission in all directions due to the existence of an omnidirectional total reflection band. However, notable improvements are expected by exploiting the 3D symmetry enhancement using postprocessing techniques.

We thank L. F. Marsal and J. Ferré-Borrull from the Universitat Rovira i Virgili for discussions and technical support. M.G. acknowledges fellowship support from DURSI of Catalonia's Government and from the European Social Fund. T.T. acknowledges support from the Spanish Government for a Juan de la Cierva fellowship. This work has been funded by the Spanish Government through CICYT-TEC2005-02716/MIC.

[1] J. F. Waymouth, U.S. Patent No. 5,079,473 (January 7, 1992).
[2] S. Y. Lin, J. Moreno, and J. G. Fleming, Appl. Phys. Lett. **83**, 380 (2003).
[3] E. Yablonovitch, Phys. Rev. Lett. **58**, 2059 (1987).
[4] M. Laroche, R. Carminati, and J.-J. Greffet, Phys. Rev. Lett. **96**, 123903 (2006).
[5] S. Y. Lin, J. G. Fleming, E. Chow, and Jim Bur, Phys. Rev. B **62**, R2243 (2000).
[6] J.-H. Lee, Y.-S. Kim, D. Constant, and K.-M. Ho, Adv. Mater. (Weinheim, Ger.) **19**, 791 (2007).
[7] V. Lehmann, J. Electrochem. Soc. **140**, 2836 (1993).
[8] J. Schilling, A. Birner, F. Müller, R. B. Wehrspohn, R. Hillebrand, U. Gösele, K. Busch, S. John, S. W. Leonard, and H. M. van Driel, Opt. Mater. (Amsterdam, Neth.) **17**, 7 (2001).
[9] S. Matthias, F. Müller, C. Jamois, R. B. Wehrspohn, and U. Gösele, Adv. Mater. (Weinheim, Ger.) **16**, 2166 (2004).
[10] S. W. Leonard, H. M. van Driel, A. Birner, U. Gösele, and P. R. Villeneuve, Opt. Lett. **25**, 1550 (2000).
[11] G. Mertens, R. B. Wehrspohn, H. S. Kitzerow, S. Matthias, C. Jamois, and U. Gösele, Appl. Phys. Lett. **87**, 241108 (2005).
[12] W. Konz, J. Hildenbrand, M. Bauersfeld, S. Hartwig, A. Lambrecht, and V. Lehman, Proc. SPIE **5836**, 540 (2005).
[13] T. Trifonov, M. Garín, A. Rodríguez, L. F. Marsal, and R. Alcubilla, Phys. Status Solidi A **204**, 3237 (2007).
[14] J. Schilling, F. Müller, S. Matthias, R. B. Wehrspohn, U. Gösele, and K. Busch, Appl. Phys. Lett. **78**, 1180 (2001).
[15] S. Johnson and J. D. Joannopoulos, Opt. Express **8**, 173 (2001).
[16] E. Lindermeier, P. Haschberger, V. Tank, and H. Dietl, Appl. Opt. **31**, 4527 (1992).